

## using a screening multi-tumor tissue microarray and rapid multiplex fluorescence digital phenotyping approach

Marie Cumberbatch<sup>1</sup>, Douglas Wood<sup>2</sup>, Gourab Chatterjee<sup>2</sup>, Christopher Womack<sup>1</sup>, Milan Bhagat<sup>1</sup>, Lorcan Sherry<sup>3</sup><sup>1</sup>TriStar Technology Group, LLC, 1901 Pennsylvania Ave NW, Washington, DC 20006, USA, <sup>2</sup>Ultivue, Inc, 763D Concord Ave, Cambridge MA 02138, USA, <sup>3</sup>OracleBio, BioCity Scotland, Bo'Ness Road, North Lanarkshire, ML1 5UH, Scotland, UK

## background

Programmed death ligand-1 (PD-L1) contributes to immune suppression in the tumor microenvironment (TME) by interacting with programmed cell death-1 (PD-1) on infiltrating T lymphocytes leading to tumor immune escape. Application of omics technologies has shed light on the relevance of the TME for response to immunotherapies and development of novel treatment options. Here we have applied a multi-plex immunofluorescence/multi-tumor tissue microarray (TMA) approach to examine the immunobiology of different TMEs with respect to the contribution by tumor cells and macrophages to overall PD-L1 expression.

## methods

A TMA comprising 11 tumour types and a total of 144 different donors, each represented by two cores [1mm; 1 from invasive margin (IM) and 1 from tumor center (TC)], was stained using Ultivue's Immuno8 FixVUE™ panel (CD3, CD4, CD8, FOXP3, CD68, PD-1, PD-L1, pan-CK/SOX10). Whole slide images from two rounds of imaging (x20 magnification; four markers in each round) were aligned using UltiStacker® software based on the nuclear counterstains from the two imaging rounds, to provide precise marker colocalization data (Figure 1). A Deep Learning algorithm was developed in Visiopharm™ software to initially classify tumor/stroma regions of interest (ROI) per core using the pan-CK/SOX10 and DAPI stain layers. A separate algorithm was then developed to segment cells and generate cell phenotype data for each of the 288 cores.

## results

- Total PD-L1 positivity (tumor plus macrophage) was greatest for NSCLC, SCLC, TNBC and gastric cancer with values ranging from approx. 600-1000 PD-L1+ cells/mm<sup>2</sup>/core. Lower values in the range approx. 50-300 PD-L1+ cells/mm<sup>2</sup>/core were observed for pancreatic, breast, liver, and gastric esophageal junction (GOJ) cancers (Figure 2A). Contribution by macrophages to overall PD-L1 expression (dual CD68+/PD-L1+) varied by tumor type representing 25-35% for NSCLC (SCC and ADC) and gastric cancer, whereas a converse pattern was apparent for SCLC, TNBC, CRC, breast (ER+ and Her2+) and pancreatic cancers where PD-L1+ macrophages accounted for a large proportion (approx. 60-85%) of overall tumor PD-L1 expression (Figure 2B).
- Interestingly, as a proportion of total macrophage infiltration, approximately 65% of CD68+ macrophages were PD-L1+ for SCLC and TNBC, compared with less than 10% for pancreatic and liver cancer (Figure 3).
- In general, the distribution of PD-L1+ macrophages between tumor (CK+) and stroma (CK-) remained approximately similar for both compartments across tumor types (Figure 4), despite a striking exclusion of CD3+/CD8+ cytotoxic T cells (CTLs) from CK+ tumor regions for some cancers such as pancreatic and liver cancer. These analyses revealed PD-L1+ macrophages to have a more dominant presence relative to CTLs for breast and lung cancers compared with gastrointestinal tumors.

## conclusions

- Taken together, these data illustrate the benefits of combining multiplexed immunofluorescence staining, with digital analysis of cell phenotypes within well characterized tumor samples to better understand the relative immunobiology of different TMEs.
- Here we demonstrate that the relative contribution of macrophages to the overall PD-L1 microenvironment varies between tumor types, which may help guide options for successful immunotherapy strategies.

Multiplex digital phenotyping across immuno-oncology screening TMA Figure 1

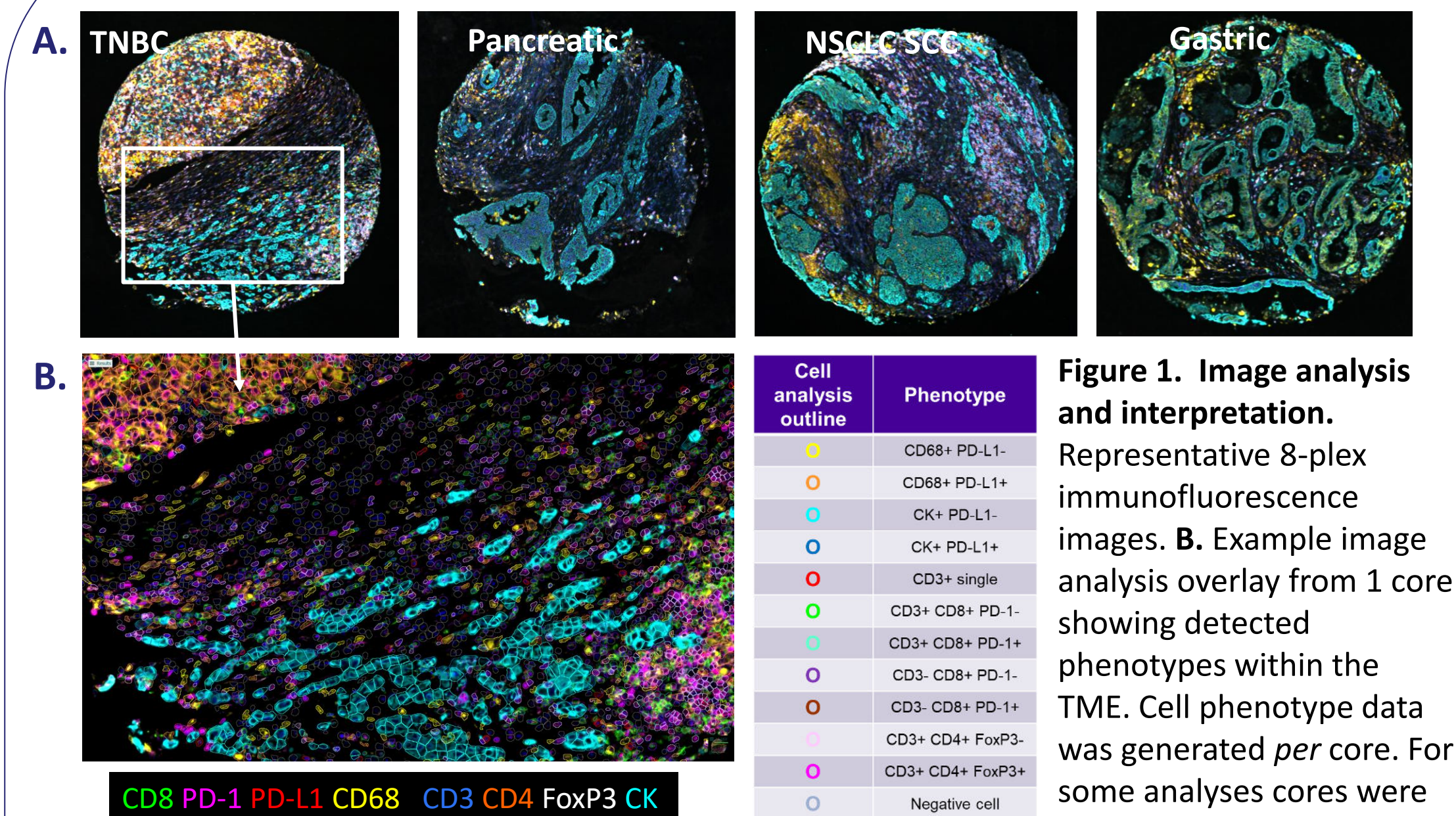


Figure 1. Image analysis and interpretation.

Representative 8-plex immunofluorescence images. B. Example image analysis overlay from 1 core showing detected phenotypes within the TME. Cell phenotype data was generated per core. For some analyses cores were segmented into CK+ tumor & CK- stroma.

Contribution of macrophages to overall PD-L1 positivity Figure 2

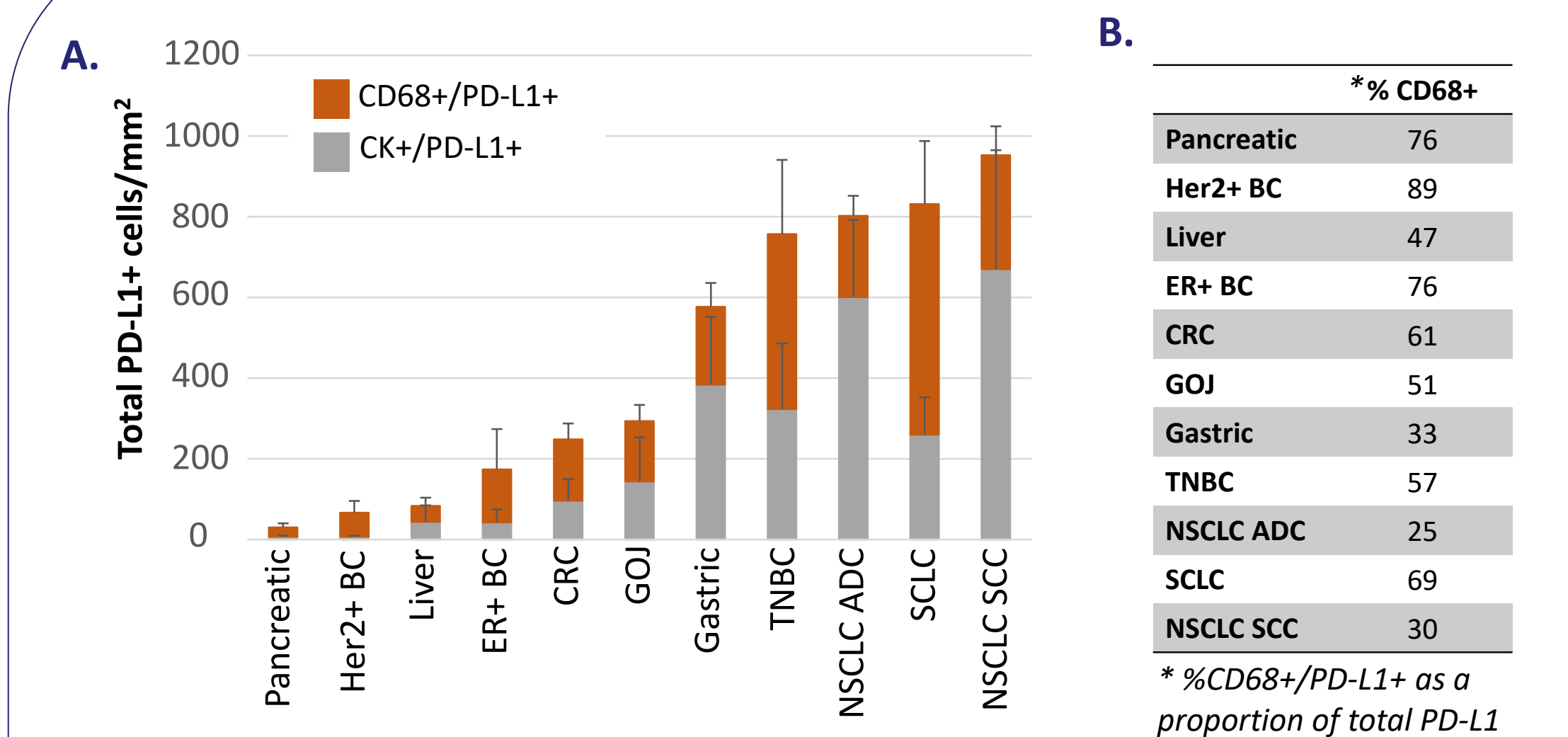


Figure 2. Relative contribution of macrophages and tumor cells to PD-L1 in the TME.

A. PD-L1+ macrophages (CD68+) and PD-L1+ tumor cells (CK+) were enumerated per core and data displayed as mean ( $\pm$ SE) values for all cores regardless of location (IM/TC) for each tumor type. Data are plotted in increasing order with respect to total PD-L1+ content. B. Contribution of CD68+ macrophages to total TME PD-L1 expression (%).

Involvement of macrophages in the TME Figure 3

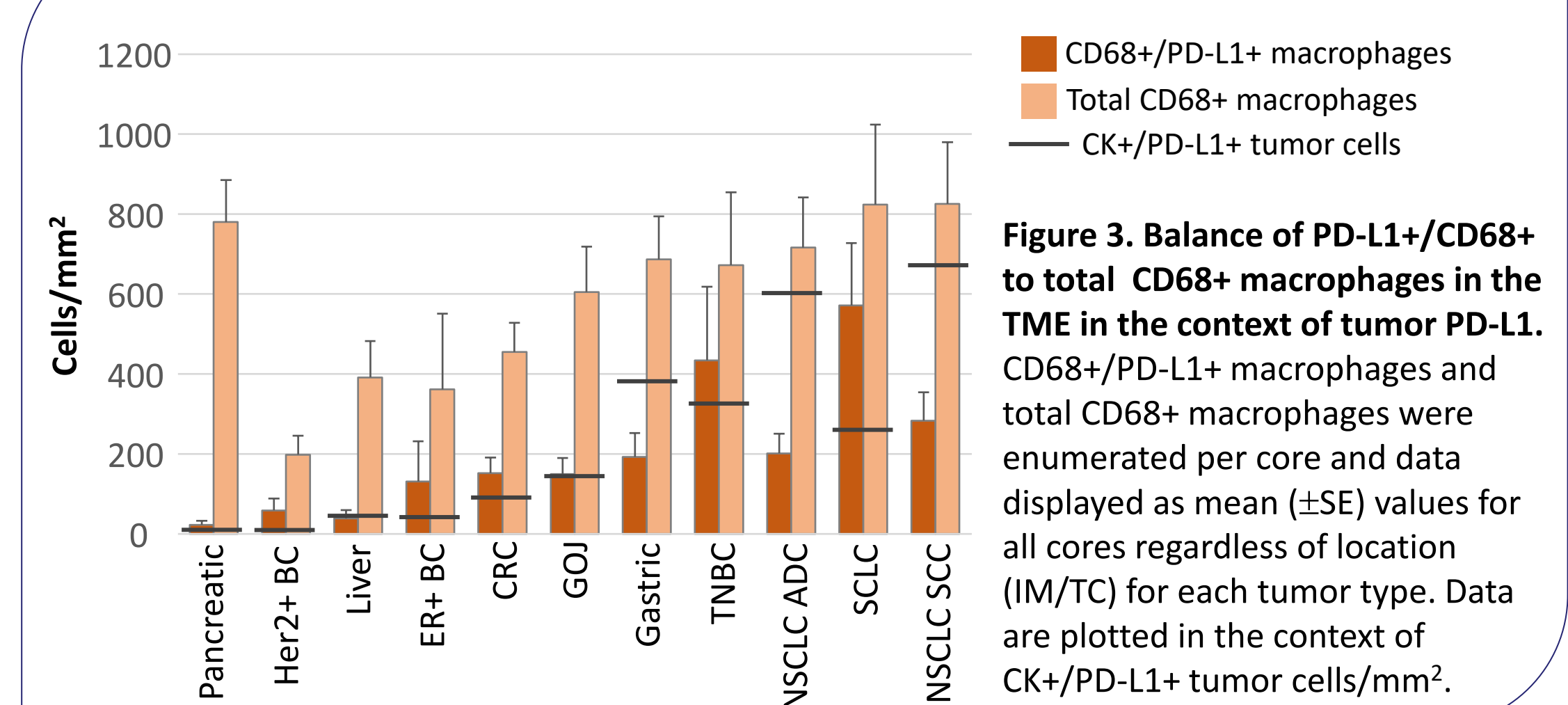


Figure 3. Balance of PD-L1+/CD68+ to total CD68+ macrophages in the TME in the context of tumor PD-L1. CD68+/PD-L1+ macrophages and total CD68+ macrophages were enumerated per core and data displayed as mean ( $\pm$ SE) values for all cores regardless of location (IM/TC) for each tumor type. Data are plotted in the context of CK+/PD-L1+ tumor cells/mm<sup>2</sup>.

Spatial analysis of PD-L1+ macrophages in tumor vs stroma: comparison with CTLs Figure 4

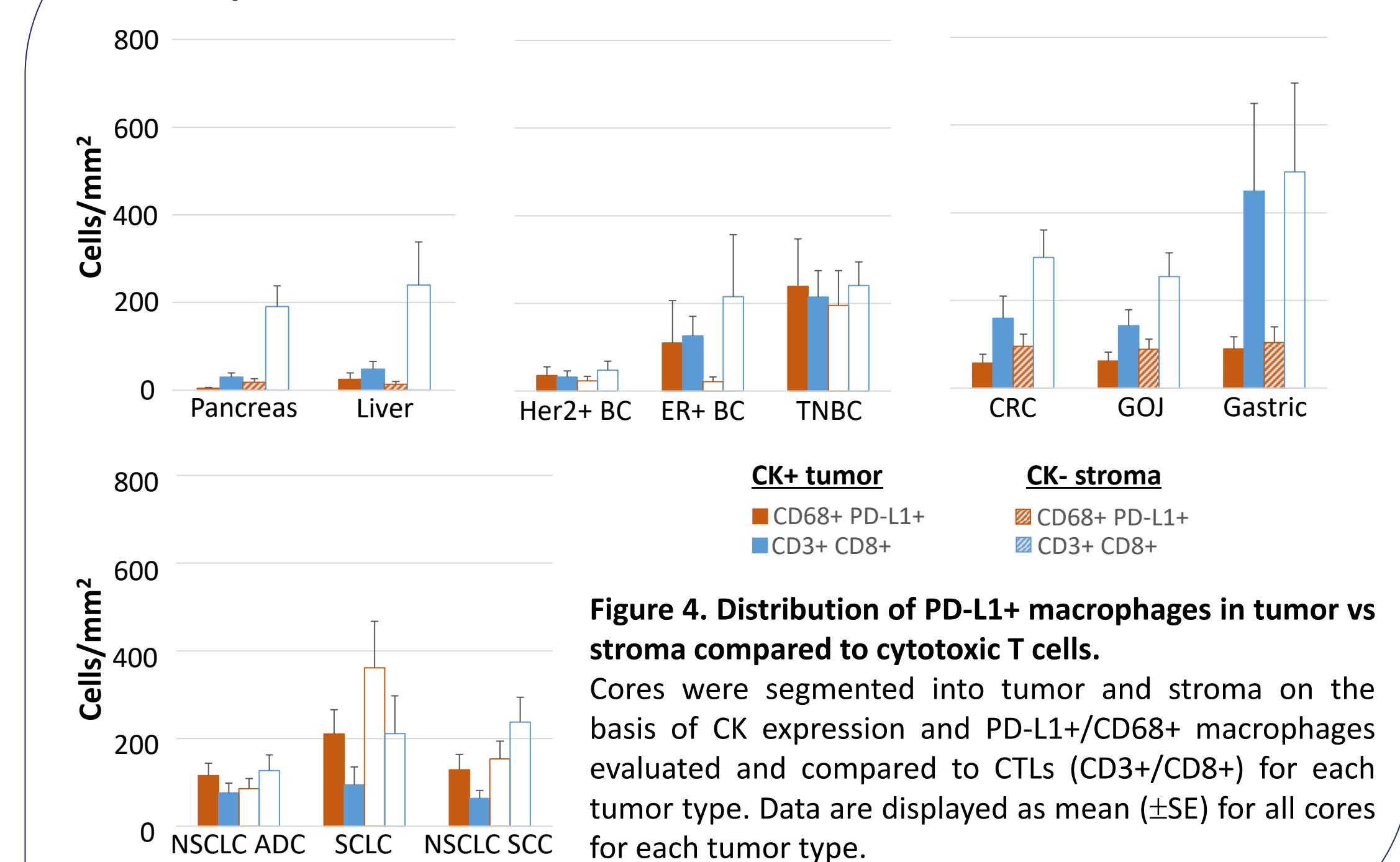


Figure 4. Distribution of PD-L1+ macrophages in tumor vs stroma compared to cytotoxic T cells.

Cores were segmented into tumor and stroma on the basis of CK expression and PD-L1+/CD68+ macrophages evaluated and compared to CTLs (CD3+/CD8+) for each tumor type. Data are displayed as mean ( $\pm$ SE) for all cores for each tumor type.